Cardiovascular Research (2015) **107**, 431–441
doi:10.1093/cvr/cvv173

Dermcidin: a skeletal muscle myokine modulating cardiomyocyte survival and infarct size after coronary artery ligation

Giovanni Esposito[1†*], Gabriele Giacomo Schiattarella[1†‡], Cinzia Perrino[1†], Fabio Cattaneo[1], Gianluigi Pironti[1,2], Anna Franzone[1], Giuseppe Gargiulo[1], Fabio Magliulo[1], Federica Serino[1], Giuseppe Carotenuto[1], Anna Sannino[1], Federica Ilardi[1], Fernando Scudiero[1], Linda Brevetti[1], Marco Oliveti[1], Giuseppe Giugliano[3], Carmine Del Giudice[1], Michele Ciccarelli[4], Giovanni Renzone[5], Andrea Scaloni[5], Nicola Zambrano[6], and Bruno Trimarco[1]

[1]Division of Cardiology, Department of Advanced Biomedical Sciences, Federico II University, Via Pansini 5, Naples 80131, Italy; [2]Department of Medicine, Duke University Medical Center, Durham, USA; [3]Montevergine Clinic, Mercogliano, Italy; [4]Department of Medicine and Surgery, University of Salerno, Naples, Italy; [5]Proteomics & Mass Spectrometry Laboratory, ISPAAM, National Research Council, Naples, Italy; and [6]Department of Molecular Medicine and Medical Biotechnologies/CEINGE-Advanced Biotechnology, Federico II University, Naples, Italy

Received 9 September 2014; revised 16 May 2015; accepted 5 June 2015; online publish-ahead-of-print 22 June 2015

Time for primary review: 35 days

Aims Coronary artery disease is the leading cause of death in western countries, and its association with lower extremity peripheral artery disease (LE-PAD) represents an independent predictor of worse outcome. However, the molecular mechanisms underlying these effects are currently unknown.

Methods and results To investigate these processes, we used *in vitro* approaches and several mouse models: (i) unilateral limb ischaemia by left common femoral artery ligation [peripheral ischaemia (PI), $n = 38$]; (ii) myocardial infarction by permanent ligation of the left descending coronary artery (MI, $n = 40$); (iii) MI after 5 weeks of limb ischaemia (PI + MI, $n = 44$); (iv) sham operation (SHAM, $n = 20$). Compared with MI, PI + MI hearts were characterized by a significant increase in cardiomyocyte apoptosis, larger infarct areas, and decreased cardiac function. By using a proteomic approach, we identified a ≅8 kDa circulating peptide, Dermcidin (DCD), secreted by ischaemic skeletal muscles, enhancing cardiomyocytes apoptosis under hypoxic conditions and infarct size after permanent coronary artery ligation. siRNA interference experiments to reduce DCD circulating levels significantly reduced infarct size and ameliorated cardiac function after MI.

Conclusion Our data demonstrate that chronic limb ischaemia activates detrimental pathways in the ischaemic heart through humoral mechanisms of remote organ crosstalk. Thus, DCD may represent a novel important myokine modulating cardiomyocyte survival and function.

Keywords Myocardial ischemia • Peripheral artery disease • Dermicidin • Apoptosis • Cardiomyocytes

1. Introduction

Coronary artery disease (CAD) is an important clinical manifestation of systemic atherosclerosis and represents the first cause of death in industrialized countries.[1] In CAD patients, abrupt coronary occlusion determines a permanent loss of cardiac myocytes, and infarct size is one of the major determinants of subsequent pathological cardiac remodelling and heart failure.[2] Experimental inhibition of programmed cell death during the acute phase of myocardial ischaemia can reduce the extension of the infarct area and, in turn, ameliorate post-ischaemic cardiac dysfunction and prolong survival.[2]

In patients with established CAD, large clinical studies have previously shown that the coexistence of lower extremity peripheral artery disease (LE-PAD) causes a worsening of the clinical course and

* Corresponding author. Tel/fax: +39 081 7463075, Email: espogiov@unina.it

† First three authors equally contributed to this work.

‡ Present address. Department of Internal Medicine (Cardiology), University of Texas Southwestern Medical Center, Dallas, TX 75390-8573, USA.

prognosis.[3] In addition, LE-PAD patients were demonstrated to have a three- to six-fold higher risk of cardiovascular events than those with similar risk factors, but without lower extremity ischaemia.[3,4] The increased vulnerability to cardiovascular (CV) events in patients with CAD can be partially explained by shared CV risk factors and excess inflammation indicated by significantly higher serum levels of inflammatory bio-markers in LE-PAD population.[5,6] However, this assumption has been recently challenged, since in patients with CAD, concomitant LE-PAD does not necessarily entail a more severe coronary atherosclerosis,[3] and only patients with an active inflammatory status of the affected limb present severe CAD[3] or coronary artery endothelial dysfunction.[7] Thus, the mechanisms underlying these synergistic detrimental effects are currently unknown.

Previous observations have reported that skeletal muscle metabolism can cause the local generation of cytokines that can be detected in the serum and may exert either systemic and/or paracrine effects.[8] Although muscle cells might not exclusively secrete these factors, they are usually classified as 'myokines' within the context of skeletal muscle physiology. Emerging evidence suggests that these muscle-derived molecules play an important role in mediating both acute metabolic changes, as well as the long-term metabolic regulatory mechanisms in distant organs like the adipose tissue and liver.[9]

Thus, in the present study, we tested the hypothesis that ischaemic skeletal muscles might produce and release into the bloodstream soluble molecules exerting remote effects on cardiomyocyte survival/functionality. To unveil the molecular signals involved in the crosstalk between ischaemic skeletal muscles and the heart, we investigated with proteomic procedures two well-established murine models of cardiac and/or peripheral ischaemia (PI) induced by permanent coronary and/or femoral arteries ligation. Here, we identify the skeletal muscle-secreted peptide Dermcidin (DCD) as a novel molecular signal underlying the remote crosstalk between the skeletal muscles and the heart.

2. Methods

An expanded Methods section is given in the Supplementary material online.

2.1 Animal studies

All experiments involving animals in this study conformed to the Guide for the Care and Use of Laboratory Animals published by the US National Institutes of Health (NIH Publication 8th edition, update 2011), and were approved by the animal welfare regulation of the University of Naples Federico II, Italy. Details are provided in Supplementary material online.

2.2 Mouse model of myocardial infarction

Mice were anaesthetized with an intraperitoneal injection of 1 mL/kg (50 mg/kg) of a mixture of 50% tiletamine and 50% zolazepam (50 mg/mL tiletamine and 50 mg/mL zolazepam, Zoletil 100), plus xylazine 5 mg/kg (Sigma-Aldrich). The adequacy of anaesthesia was confirmed by the absence of reflex response to foot squeeze. Myocardial infarction (MI, $n = 40$) was induced in mice by permanent ligation of the left coronary artery, as previously described.[10] Details are provided in Supplementary material online.

2.3 Mouse model of chronic hindlimb ischaemia

Hindlimb ischaemia (PI, $n = 38$) was induced in mice as previously described.[11,12] Details are provided in Supplementary material online. After 5 weeks of hindlimb ischaemia, an additional group of PI mice underwent myocardial infarction as described earlier (PI + MI, $n = 44$).

2.4 Transthoracic echocardiography

Cardiac function was non-invasively monitored by transthoracic echocardiography by using a Vevo 770 high-resolution imaging system (VisualSonics, Toronto, Canada) before the surgery and right before termination, 7 days after myocardial infarction as previously described.[13] Details are provided in Supplementary material online.

2.5 Measurement of blood pressure and cardiac function

Systolic blood pressure (SBP) and diastolic blood pressure (DBP) were measured in conscious mice from different experimental groups using a non-invasive computerized tail-cuff system (Visitech Systems, Apex, NC, USA) as described previously.[14,15] Details are provided in Supplementary material online.

2.6 Morphological studies

Mouse heart specimens fixed in 4% formaldehyde were embedded in paraffin; after de-paraffinization and re-hydratation, 4 μm-thick sections were prepared, mounted on glass slides and stained with Haematoxylin–Eosin, Sirius red, lectin, or Terminal deoxynucleotidyl transferase dUTP nick end labelling (TUNEL). Details are provided in Supplementary material online.

2.7 Cell cultures, *in vitro* hypoxia, and lactate dehydrogenase measurement

Primary cultures of neonatal ventricular myocytes (NVMs) were prepared from 1/3-day-old Wistar rats sacrificed by cervical dislocation followed by decapitation, as previously described.[16] NVMs were cultured in serum-free conditions for 48 h before experiments, and then incubated with 1:50 dilution of serum from SHAM, PI, MI, and PI + MI animals, under normoxic or hypoxic conditions (discussed subsequently), for 4 h. In additional experiments, NVMs were incubated with the tagged fusion DCD peptide corresponding to amino acids 20–110 (Santa Cruz Biotechnology) under normoxic and hypoxic conditions. Details are provided in Supplementary material online. Hypoxia (2% O_2) was induced when NVMs were at 0.85 confluence. Details are provided in Supplementary material online. Lactate dehydrogenase (LDH) levels in NVMs supernatants from different experimental groups were determined by using LDH assay kit (Abcam) according to the manufacturer's instructions.

2.8 Immunodepletion assay

For immunodepletion experiments, serum samples from SHAM and PI were incubated twice with a polyclonal rabbit antibody against DCD (3 μg, Santa Cruz Biotechnology) or control IgG (3 μg, Santa Cruz Biotechnology) for 1 h, at 4°C, and incubated with 20 μL of protein G-agarose beads (GIBCO-BRL) on a roller system, for another 1 h, at 4°C. Details are provided in Supplementary material online.

2.9 Annexin V and propidium iodide staining

Cultured cells were rinsed with ice-cold phosphate-buffered saline (PBS), fixed with 3.7% formaldehyde in PBS for 30 min, permeabilized with 0.2% Triton X-100 in PBS, and then incubated with 2% bovine serum albumin in PBS for 1 h, at room temperature. In order to evaluate apoptotic cell death, cultured cells were stained with Annexin V Cy3 (MBL, Japan) and propidium iodide (P) (Sigma-Aldrich), and the percentage of apoptosis was analysed by fluorescence microscopy or by flow cytometry (Epics XL, Beckman Coulter). Further details are provided in Supplementary material online.

2.10 Protein extraction, immunoblot analysis, immunohistochemistry, and immunofluorescence

Cultured cells and left-ventricular samples were lysed and immunoblotting was performed by using commercially available antibodies anti-DCD (rabbit polyclonal, Santa Cruz), PARP (mouse monoclonal, Santa Cruz), Caspase-3 (rabbit polyclonal, Cell Signaling), cleaved Caspase-3 (rabbit polyclonal, Cell Signaling) α-heavy chain myosin (α-MHC, mouse monoclonal, Abcam), and GAPDH (mouse monoclonal, Upstate Biotechnology). α-MHC immunostaining were performed on 4 μm-thick deparaffinized and rehydrated through decreasing ethanol concentrations heart sections. Details are provided in Supplementary material online.

2.11 Bio-plex cytokines assay

Tumour necrosis factor α (TNF-α), Interleukin 1β (IL-1β) and Interleukin 6 (IL-6) activation was evaluated in sera from SHAM, MI, and PI mice by Bio-Plex cytokine assay (Bio-Rad) according to the manufacturer's instructions and as previously described.[17]

2.12 Serum fractionation and mass spectrometric analysis

Sera from SHAM and PI mice were subjected to subfractionation by using 10 kDa Spin Column devices (Amicon, Millipore) to isolate a protein subfraction with components having molecular mass <10 kDa (SHAM < 10 kDa or PI < 10 kDa) or a protein subfraction with components having molecular mass >10 kDa (SHAM > 10 kDa or PI > 10 kDa). Next, sera SHAM < 10 kDa or PI < 10 kDa were subjected to high-pressure liquid chromatography (HPLC) fractionation on a C_{18} Jupiter column (250 × 2.1 mm, 5 μm Phenomenex) eluted with a linear gradient (from 5 to 75%) of 0.1% trifluoroacetic acid, acetonitrile in 0.1% trifluoroacetic acid over 70 min, at a flow rate 0.2 mL/min. After sample injection, fraction collection was set up to continuously accumulate portions of 0.4 mL each, which were then lyophilized and further subjected to the apoptotic assays reported earlier and/or to MS analysis. Details are provided in Supplementary material online.

2.13 RNA extraction, cDNA synthesis, real-time PCR, and sequence alignment

Total RNA was prepared by using the TRIzol procedure (Invitrogen, Eugene, OR, USA), according to the manufacturer's instruction. Oligo-dT first strands cDNA were synthesized using the SuperScript VILO cDNA Synthesis (Invitrogen, Life technologies) according to the manufacturer's instructions.

DCD mRNA expression was determined in cardiac and skeletal muscles by quantitative real-time PCR (RT-PCR) using a IQ-5 Multicolor Real-Time PCR detection system (Bio-Rad). The primers used are listed in *Table 1*. The initial denaturation phase was performed at 95°C for 5 min, followed by an amplification phase as detailed in what follows: denaturation at 95°C for 10 s; annealing at 60°C for 30 s; elongation at 72°C for 30 s; detection at 72°C for 40 cycles.

DCD amino acid and cDNA sequences were obtained by sequence service at CEINGE-Advanced Biotechnology, Federico II University, Naples, Italy and alignment were performed by the web-accessible ClustalW2 tool.

2.14 siRNA studies

DCD expression knockdown in mice was obtained by using a small-interfering RNA (siRNA) synthesized by Santa Cruz (siDCD). Forty-eight hours before coronary artery ligation, siDCD (30 nmol/kg) or negative, fluorescein isothiocyanate (FITC)-conjugated control siRNA (siCTR) (660 mmol/mouse) (Santa Cruz) diluted in PBS were injected in PI + MI mice via the tail vein (PI + MI siDCD, $n = 10$ and PI + MI siCTR, $n = 6$), as previously described.[18] Efficacy of siRNA approach was evaluated by visualizing FITC-expression in the skeletal muscle sections by green fluorescence.

2.15 Statistical analysis

All data are reported as mean ± SEM. Comparisons between two groups were performed using the unpaired Student's *t*-test. For four groups experiments, comparisons were made by two-way analysis of variance (ANOVA). Correction for multiple comparisons was made using the Student–Newman–Keuls method. A *P*-value of <0.05 was considered statistically significant. All the analyses were performed with the GraphPad Prism version 5.01 (GraphPad Software, San Diego, CA, USA).

3. Results

3.1 Chronic hindlimb ischaemia enhances apoptotic cardiomyocyte death and increases infarct size after coronary artery ligation in mice

To address the molecular mechanisms underlying the possible interplay between limbs and cardiac ischaemia *in vivo*, two murine models of cardiac or PI were used. To induce chronic limb ischaemia, C57BL/6 mice ($n = 82$) underwent 5 weeks of femoral artery ligation (PI), as previously described.[11,12] In some PI mice ($n = 44$), after 5 weeks of hindlimb ischaemia, myocardial infarction was induced by permanent coronary artery ligation (PI + MI) as previously described.[10] In an additional group of mice ($n = 40$), only coronary artery ligation was performed (MI). SHAM-operated animals ($n = 20$) underwent the same surgical procedures without ligation of the femoral or coronary arteries. Twenty-four hours following permanent coronary artery ligation, MI or PI + MI hearts ($n = 7$ and $n = 8$, respectively) were infused with Evans blue to demarcate the ischaemic area susceptible to infarction [area at risk (AAR)], and counterstained with triphenyltetrazolium chloride to identify the infarct area (IA) from the viable myocardium within the AAR. Despite similar AARs between the two MI groups (*Table 2*), PI + MI hearts demonstrated a significantly larger proportion of infarcted myocardium within the AAR, when compared with MI mice (*Table 2* and *Figure 1A*). Seven days after coronary artery ligation, PI + MI hearts still displayed a significantly larger infarct size by Sirius red staining compared with MI (*Figure 1B*), suggesting that chronic

Table 1 DNA primers used in the study

GENE	Forward	Reverse
DCD	5′-GTTAGCCAGACAGGCACCA-3′	5′-CTCCGTCTAGGCCTTTTTCC-3′
GAPDH	5′-TGCAGTGGCAAAGTGGAGATT-3′	5′-TCGCTCCTGGAAGATGGTGAT-3′

hindlimb ischaemia at the time of coronary artery occlusion might enhance the detrimental actions of cardiac ischaemia.

Next, to evaluate the effects of these different conditions on cardiac function, transthoracic echocardiography was performed in the different groups (*Figure 1C*). As expected, while coronary artery ligation produced myocardial infarction and a significant reduction of cardiac function, chronic limb ischaemia did not affect cardiac function under normal conditions (*Figure 1C* and *Table 3*). Interestingly, compared with MI, PI + MI mice displayed a significant worsening in cardiac function after coronary artery ligation, and a more pronounced increase in the left-ventricular weight (LVW) to body weight (BW) ratio at study termination without a significant increase in end-diastolic wall thicknesses of either the interventricular septum (IVSd) or the posterior wall (PW), consistent with an expansion of the infarct region and/or increased oedema in the remote region (*Table 3*). These data suggest that the contemporary presence of skeletal muscle ischaemia might aggravate cardiac response to coronary artery occlusion. Moreover, there was no significant change in systolic blood pressure (SBP), diastolic blood pressure (DBP) or heart rate (HR) in either MI or MI + PI groups (MI (mmHg): SBP = 132.7 ± 8.6, DBP = 85.3 ± 22.1; PI + MI

Table 2 Infarct area and area at risk 24 h after permanent coronary artery ligation in mice from the different experimental groups

	MI (n = 7)	PI + MI (n = 8)
IA/AAR (%)	44.8 ± 1.2	68.4 ± 3.0*
AAR/LV (%)	32.3 ± 1.3	31.4 ± 1.5

IA, infarct area; AAR, area at risk; LV, left-ventricle area.
*P < 0.05 vs. MI.

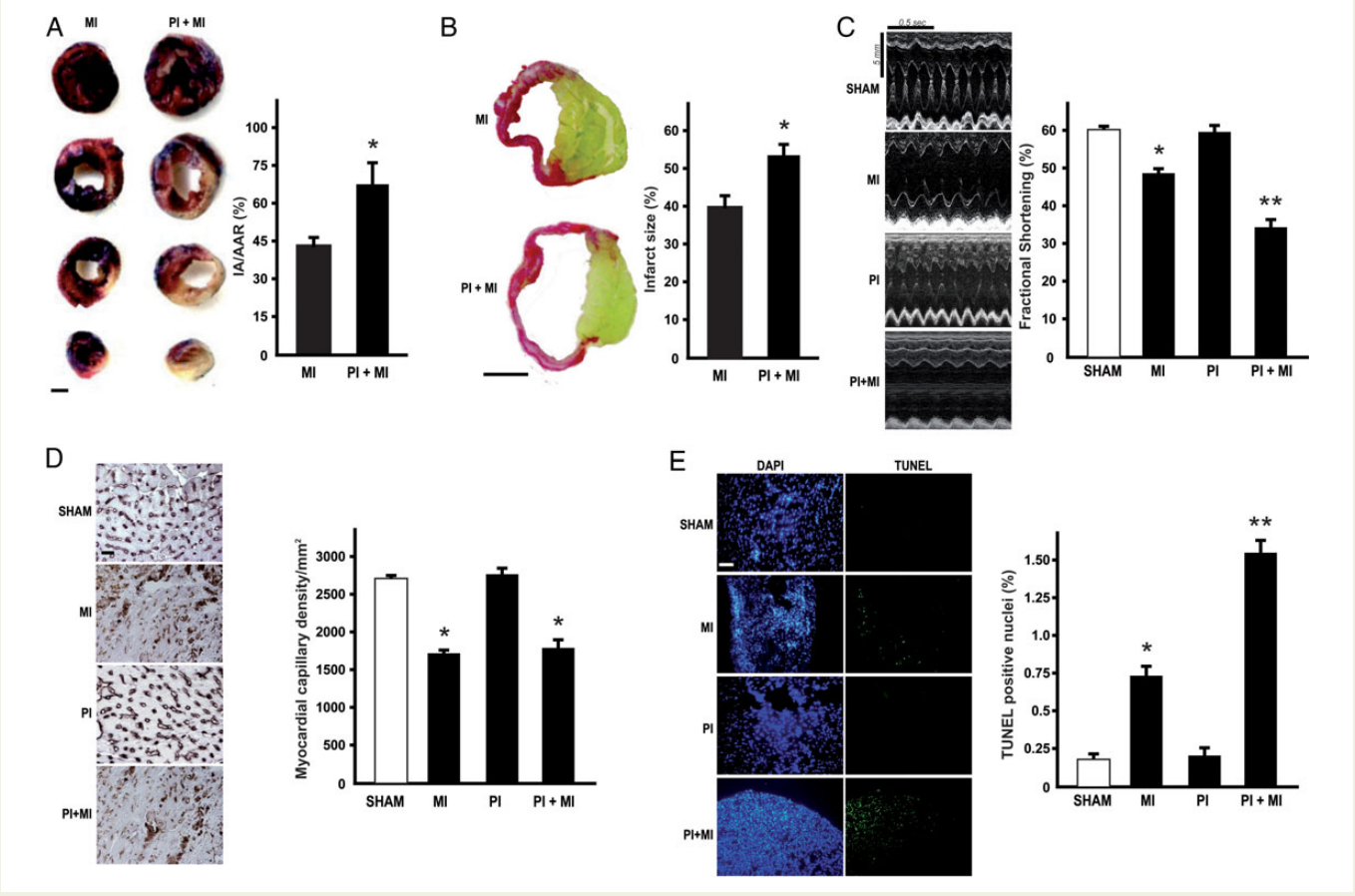

Figure 1 Cardiac evaluation of mice with chronic hindlimb ischaemia and myocardial infarction. (*A*) Left: Representative images of triphenyltetrazolium chloride (TTC) staining of cardiac sections from mice undergoing 24 h of permanent coronary artery ligation alone (MI) or 5 weeks of femoral artery ligation to induce peripheral ischaemia (PI) followed by 24-h-MI (PI + MI) (scale bar = 1 mm). Right: bar graphs showing ratios of myocardial infarct area (IA) and area at risk (AAR) in MI and PI + MI groups (*P < 0.05 vs. MI; n = 9 hearts/group). (*B*) Left: representative images of Sirius red staining of cardiac sections after 7 days of permanent coronary artery ligation alone (MI) or 5 weeks of PI followed by 7-day-MI (PI + MI) (scale bar = 2 mm). Right: bar graphs showing percent infarct size in MI and PI + MI mice (*P < 0.05 vs. MI; n = 10 hearts/group). (*C*) Left: representative M-mode echocardiographic tracings. Right: cumulative data of % fractional shortening in MI, PI, PI + MI, or SHAM mice (*P < 0.05 vs. SHAM; **P < 0.05 vs. all; n = 10 hearts/group). (*D*) Left: representative lectin staining of cardiac sections from SHAM, MI, PI, and PI + MI mice. Capillaries appear brown (scale bar = 500 nm). Right: cumulative data of multiple independent experiments analyzing capillary density in the different groups (*P < 0.05 vs. SHAM and PI; n = 7–8 hearts/group). (*E*) Left: representative DAPI and TUNEL staining of cardiac sections from SHAM, MI, PI, and PI + MI mice. TUNEL-positive nuclei appear green (scale bar = 250 nm). Right: cumulative data of multiple independent experiments (*P < 0.05 vs. SHAM and PI; **P < 0.05 vs. all, n = 7–8 hearts/group). Experiments were repeated three times and the data pooled.

Table 3 Morphometric and echocardiographic evaluation

	SHAM ($n = 20$)	PI ($n = 38$)	MI ($n = 40$)	PI + MI ($n = 44$)
BW (g)	26.8 ± 0.2	26.5 ± 0.2	26.7 ± 1.7	25.1 ± 0.4
LVW (mg)	100.1 ± 5.7	99.2 ± 5.7	144.1 ± 5.1*	162.4 ± 14.3†
LVW/BW (mg/g)	3.7 ± 0.1	3.7 ± 0.1	5.3 ± 0.2*	6.4 ± 0.5†
LVEDD (mm)	3.2 ± 0.04	3.1 ± 0.03	3.4 ± 0.11*	3.8 ± 0.19*
LVESD (mm)	1.3 ± 0.04	1.2 ± 0.02	1.7 ± 0.14*	2.4 ± 0.31†
FS (%)	59.4 ± 0.73	61.3 ± 1.65	48.6 ± 0.83*	36.7 ± 1.87†
IVSd (mm)	0.9 ± 0.03	0.9 ± 0.12	1.0 ± 0.05	1.1 ± 0.12
PWd (mm)	0.8 ± 0.02	0.8 ± 0.32	0.9 ± 0.04	0.9 ± 0.03
HR (bpm)	533 ± 13.35	528 ± 13.35	543 ± 27.28	527 ± 26.12

SHAM, sham-operated control mice; MI, myocardial infarction; BW, body weight; LVW, left-ventricular weight; LVEDD, left-ventricular end-diastolic diameter; LVESD, left-ventricular end-systolic diameter; FS, fractional shortening; IVSd, end-diastolic interventricular septum; PWd, end-diastolic posterior wall; HR, heart rate.
*$P < 0.05$ vs. SHAM.
†$P < 0.05$ vs. SHAM and MI.

(mmHg): SBP = 139.4 ± 12.6, DBP = 103.2 ± 11.6, not significant, $n = 6$ and $n = 8$, respectively).

To rule out whether abnormal vascular density might be responsible for the increased infarct size in PI + MI mice, histological studies were performed in the infarct zone to stain cardiac capillaries in all experimental groups. Notably, PI mice displayed a cardiac capillary density similar to SHAM mice (*Figure 1D*), suggesting that hindlimb ischaemia may not affect microvascular remodelling in the normal heart. As expected, coronary artery ligation induced a significant reduction in myocardial capillary density (*Figure 1D*). Importantly, when myocardial infarction was surgically induced after 5 weeks of femoral artery ligation (PI + MI mice), vascular rarefaction was similarly observed, supporting the concept that the differences observed in PI + MI mice might not be attributed to alterations in the microvasculature.

To assess whether increased apoptotic cell death might be involved in the increased infarct size observed in PI + MI mice, terminal deoxynucleotidyl transferase dUTP nick end labelling (TUNEL) staining was performed in cardiac sections from the different groups. Compared with MI, PI + MI hearts exhibited a significant increase in the rate of TUNEL-positive nuclei in the infarct zone (*Figure 1E*). Importantly, the vast majority of TUNEL-positive nuclei were localized within cardiomyocytes as shown in the Supplementary material online, *Figure S1*. Taken together, these results suggest that hindlimb ischaemia enhances cardiomyocyte apoptotic cell death induced by coronary artery ligation. Importantly, MI and MI + PI hearts displayed a significant increase in leucocytes infiltration in border zone of infarct. Conversely, SHAM and PI hearts showed no significant infiltration (Supplementary material online, *Figure S2A*). These data are consistent with the results that 5 weeks of limb ischaemia did not significantly affect the levels of the pro-inflammatory cytokines TNF-α, IL-1β, and IL-6 (Supplementary material online, *Figure S2B*), indicating that systemic inflammation might not be directly involved in these processes.

3.2 Proteomic analysis and identification of DCD as the pro-apoptotic factor in PI sera

To determine whether a secreted, circulating factor might be responsible for the detrimental cardiac effects observed in PI + MI mice, rat NVMs were incubated with equal parts of serum of mice from all experimental groups during normoxia or 4 h of hypoxia; then, apoptotic cell death was evaluated by Annexin V staining. While no significant differences were observed in normoxic conditions, hypoxic cardiomyocytes incubated with either PI or PI + MI sera exhibited a significant increase in Annexin V staining, compared with hypoxic cardiomyocytes treated with SHAM or MI sera (*Figure 2A*).

In order to determine whether chronic limb ischaemia may promote the systemic release of a circulating pro-apoptotic factor, sera from PI mice were separated by ultrafiltration in two fractions, containing polypeptide molecules having a molecular mass higher or lower than 10 kDa (PI > 10 kDa and PI < 10 kDa, respectively). The ability of both fractions to induce apoptotic cell death was next tested in hypoxic or normoxic cardiomyocytes (*Figure 2B*). Interestingly, only the PI < 10 kDa fraction significantly induced apoptosis in hypoxic cardiomyocytes similar to the whole PI serum (*Figure 2B*, panels 23, 25). Thus, an HPLC separation step was applied to the PI < 10 kDa fraction to purify the bioactive component responsible for the observed phenomenon (Supplementary material online, *Figure S3A*). Collected subfractions were tested in cardiomyocytes under normoxic or hypoxic conditions as previously described, and their apoptotic activity was evaluated by Annexin V staining. Based on this assay, only adjacent subfractions #33 and #34 were found to promote apoptotic cell death in hypoxic cardiomyocytes (Supplementary material online, *Figure S3B* and *Figure 2B*, panels 26–28). These fractions were further characterized by MALDI-TOF-MS analysis, as previously described,[19] and showed in both cases the presence of a single component with a molecular mass of about 8601 kDa (Supplementary material online, *Figure 3C*). This purified compound was further digested with trypsin and characterized for its nature by nanoLC-ESI-LIT-MS/MS as DCD (Supplementary material online, *Figure 3D*). These experiments demonstrated the unique occurrence of three mouse peptides in these fraction digests, namely LGKDAVEDLESVGK, DAVEDLESVGK, and ENAGEDPGLAR, which are identical to the sequence of the corresponding human DCD protein (Supplementary material online, *Figure S3D*). Next, to confirm DCD expression in murine skeletal muscles, we generated and sequenced DCD cDNA from RNA. Interestingly, DCD cDNA mouse sequence showed 100% homology to the human DCD mRNA (Supplementary material online, *Figure S4*). The presence of DCD in the sera of PI mice and in the

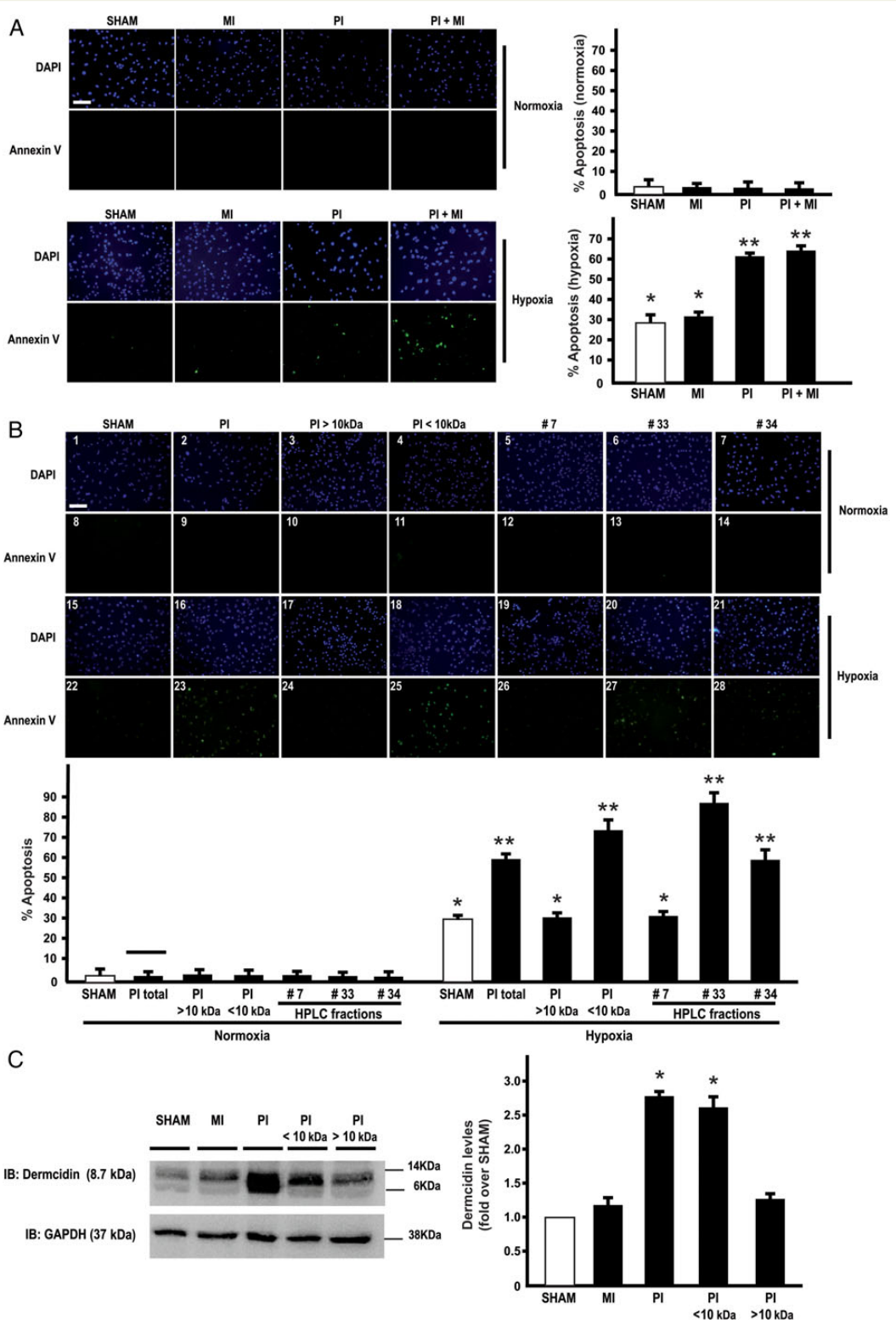

Figure 2 Proteomic identification of DCD as the pro-apoptotic factor in PI sera. (*A*) Left panels: Representative DAPI and Annexin V staining in rat NVMs incubated with sera from SHAM, MI, PI, and PI + MI mice under normoxic or hypoxic conditions. Annexin V-positive cells appear green. Scale bar = 250 μm. Right panels: cumulative data of multiple independent experiments (*$P < 0.05$ vs. normoxia; **$P < 0.05$ vs. normoxia, SHAM, and MI hypoxia; $n = 5$). (*B*) Top: representative DAPI and Annexin V staining in NVMs under normoxic or hypoxic conditions incubated with sera from SHAM or PI mice, >10 or <10 kDa polypeptide components from PI sera, fractions #7, #33, and #34 separated by HPLC analysis from PI<10 kDa sera. Annexin V-positive cells appear green. Scale bar = 250 μm. Bottom: cumulative data of multiple independent experiments (*$P < 0.05$ vs. normoxia; **$P < 0.05$ vs. all; $n = 5$). (*C*) Representative immunoblot and densitometric analysis of four independent experiments to evaluate DCD protein levels in SHAM, MI, PI, PI<10 kDa, PI>10 kDa sera (*$P < 0.05$ vs. all). GAPDH protein levels did not significantly change among the samples.

corresponding PI < 10 kDa fraction was also confirmed by immunoblotting with a specific antibody (*Figure 2C*).

3.3 DCD induces apoptosis in hypoxic cardiomyocytes

To test whether circulating plasma levels of DCD might exert detrimental effects on cardiomyocytes under normoxic or hypoxic conditions, NVMs were grown in the presence of sera from PI mice incubated with a specific DCD antibody (PI-DCD$^-$) or with control IgG (PI-DCD$^+$) (*Figure 3A*). Interestingly, while PI-DCD$^+$ sera significantly increased Annexin V staining of cardiomyocytes during hypoxia, DCD immunodepletion significantly reduced these effects (*Figure 3B*).

To discriminate between apoptosis and necrosis of cardiomyocytes, we performed double staining for P and Annexin V in isolated cardiomyocytes treated with recombinant DCD peptide under normoxic and hypoxic conditions. Interestingly, the % amount of P/annexin V staining was increased in DCD-treated hypoxic neonatal cardiomyocytes compared with hypoxic, untreated cardiomyocytes (*Figure 3C*). Moreover, treatment with recombinant DCD increased lactic dehydrogenase activity in hypoxic cardiomyocytes in the culture media (*Figure 3D*) and caspase 3/poly(ADP-ribose) polymerase (PARP) cleavage (*Figure 3E*), confirming the important role of DCD in the modulation of cell survival of cardiomyocytes upon hypoxia.

3.4 DCD regulation in skeletal and cardiac muscle

In order to assess DCD regulation in response to limb or cardiac ischaemia, expression analysis was performed on cardiac and limb muscle samples from SHAM, MI, PI, and PI + MI mice. While DCD expression in the heart was not affected by either coronary or femoral artery ligation, DCD levels in skeletal muscles significantly increased after femoral artery ligation and were unaffected by coronary artery ligation (*Figure 4A*). Consistent with these results, DCD mRNA levels were significantly increased in ischaemic skeletal limbs (*Figure 4B*), while they were unchanged in the hearts of mice undergoing femoral and/or coronary artery ligation (*Figure 4C*). Taken together, these results indicate that DCD is specifically induced in the skeletal muscle under ischaemic conditions.

3.5 *In vivo* DCD silencing reduces infarct size in mice with chronic hindlimb ischaemia

In order to test whether the increase in DCD plasma levels might be directly involved in cardiomyocyte survival during cardiac ischaemia, an *in vivo* silencing approach was undertaken by systemically administering small interfering RNA (siRNA) specific for DCD mRNA (siDCD) in PI + MI mice. Control siRNAs conjugated with fluorescein isothiocyanate - FITC (siCTR) were also administered, and visualized in limb skeletal muscles or cardiac sections by fluorescence microscopy (Supplementary material online, *Figure S5*). As expected, DCD mRNA and protein levels were significantly reduced in limb muscles from PI + MI mice treated with siDCD (*Figure 5A* and *B*). Strikingly, DCD silencing in mice with limb ischaemia significantly reduced the proportion of infarcted myocardium within the AAR after coronary artery ligation [IA/AAR (%): PI + MI siCTR: 50.3 ± 3.3; PI + MI siDCD: 64.4 ± 3.6; *$P < 0.05$, *Figure 5C*], suggesting that DCD levels might modulate infarct size after 24 h of myocardial infarction in mice with chronic limb ischaemia. Furthermore, transthoracic echocardiography performed after 7 days of coronary artery ligation showed that DCD silencing in mice with chronic limb ischaemia significantly ameliorated cardiac dysfunction after myocardial infarction (*Figure 5D*), suggesting that DCD circulating levels might modulate infarct size and post-ischaemic cardiac remodelling in mice with limb and cardiac ischaemia.

4. Discussion

In this paper, we present data on a novel molecular mechanism underlying an inter-organ communication between skeletal muscles and the heart, mediated by the muscle-secreted peptide DCD. After induction of experimental limb ischaemia, DCD was released from skeletal muscles in the systemic circulation, wherein it exerted critical effects on cardiomyocyte survival during ischaemia, enhancing infarct size and pathological cardiac remodelling after myocardial infarction. These results point at DCD as an important biomarker of skeletal muscle ischaemia, and a novel molecular target to ameliorate cardiac maladaptive responses to ischaemia.

CAD is the single largest cause of death in developed countries, and is one of the leading causes of disease burden in developing countries as well.[20] In subjects with known CAD, the simultaneous presence of any kind of peripheral artery disease represents an independent and significant predictor of death.[3,4] While it is conceivable that the coexistence of these two manifestations of atherosclerosis could be the expression, at least in part, of a more severe systemic disease,[5,6] the exceeding morbidity and mortality for cardiovascular causes in these patients has never been completely understood. Here we found that mice subjected to chronic limb ischaemia had a worse outcome after myocardial infarction, compared with animals undergoing myocardial infarction alone. Notably, since these mouse models are characterized by the absence of vascular atherosclerosis,[12] these results indicate that the detrimental cardiac effects induced by PI are independent from atherosclerosis.

It has been previously proposed that skeletal muscle secretes molecules, termed 'myokines', that might affect neighbour or remote organs through a variety of mechanisms.[8] In particular, PI might be able to induce the release of factors, such as TNF-α or similar cytokines with cardiodepressant actions.[21] However, in the present study, no differences in the circulating levels of major inflammatory cytokines or myocardial inflammatory infiltrate were observed between SHAM and PI mice (Supplementary material online, *Figure S2*), suggesting that inflammation might not be the prominent mediator of the remote crosstalk between skeletal muscles and the heart.

Remarkably, a proteomic analysis of sera from animals subjected to femoral artery ligation identified the specific peptide DCD as the crucial factor responsible for induction of apoptosis in hypoxic cardiomyocytes. DCD was originally identified in 2001 as an antimicrobial peptide with a broad spectrum of activity, constitutively expressed and secreted by sweat glands.[22] Subsequently, DCD expression has been demonstrated in a wide spectrum of tissues and cell lines.[23,24,25,26] While there is now a large amount of data concerning the role of DCD in cancer, its effects in cardiovascular pathophysiology are much less defined. Recent studies have demonstrated increased DCD serum levels in patients with acute coronary syndromes and arterial hypertension.[27,28] The same authors have also shown that DCD can increase platelets aggregation, suggesting a potential role of DCD in artery thrombosis.[27,28] Here we found that DCD relapsed by ischaemic skeletal muscles in

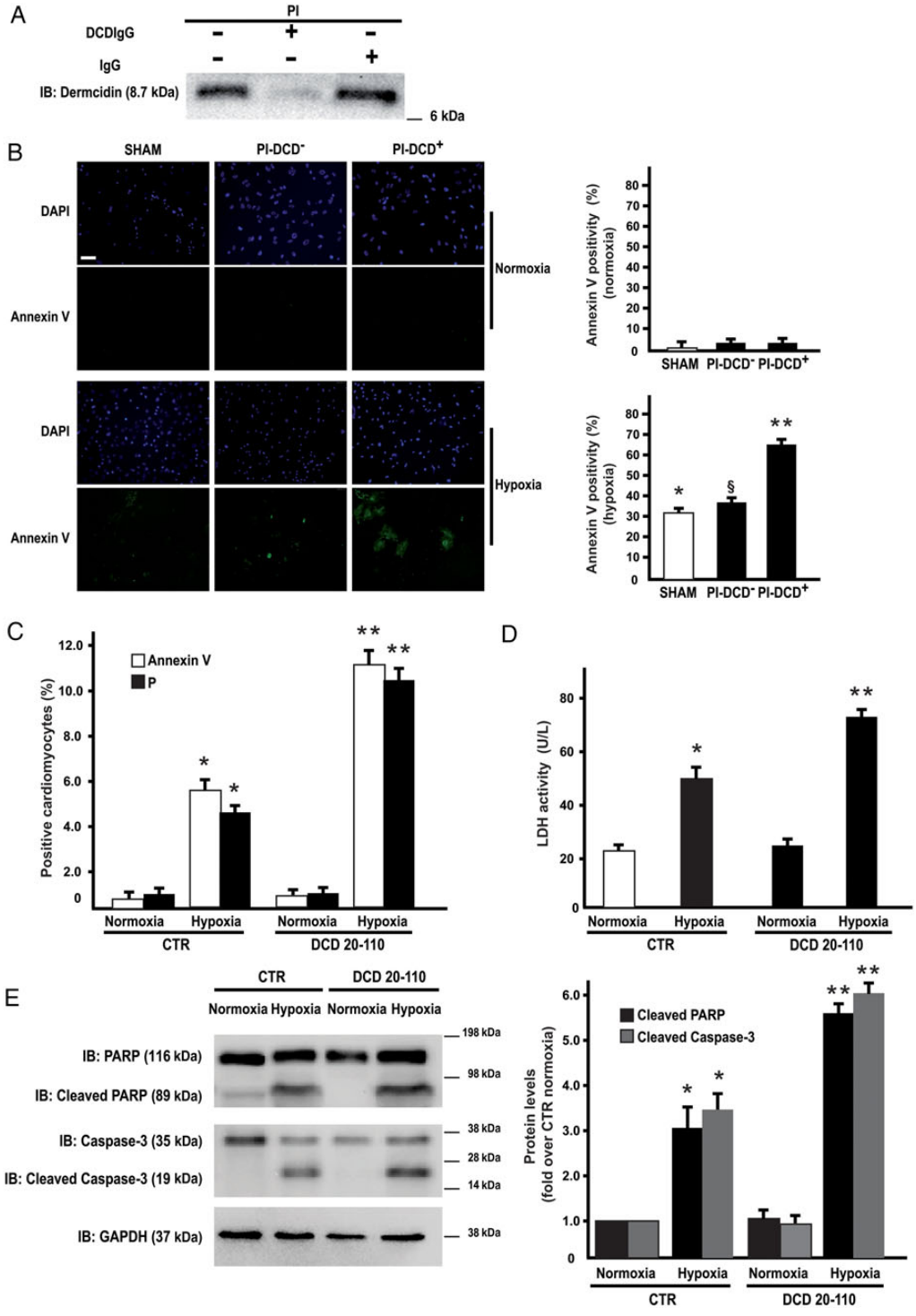

Figure 3 Cardiomyocyte apoptosis induced by DCD. (*A*) Top: representative immunoblot of four independent experiments to evaluate DCD protein immunodepletion in PI sera. DCDIgG indicates serum immunodepleted with DCD antibody and IgG indicates serum immunodepleted with control immunoglobulin. (*B*) Left panels: representative DAPI and Annexin V staining in rat NVMs under normoxic or hypoxic conditions incubated with sera from SHAM mice, or from PI mice incubated with specific anti-DCD antibody (PI-DCD$^-$) or non-specific IgG (PI-DCD$^+$). Annexin V-positive nuclei appear green. Scale bar = 250 μm. Right panels: cumulative data of four multiple independent experiments (*$P < 0.05$ vs. normoxia; **$P < 0.05$ vs. normoxia and SHAM hypoxia; §$P < 0.05$ vs. all). Scale bar = 250 μm. (*C*) Double staining for Annexin V and P in NVMs incubated with a synthetic DCD peptide (DCD 20–110) or a control peptide (CTR) under normoxic or hypoxic conditions (*$P < 0.05$ vs. normoxia; **$P < 0.05$ vs. all). (*D*) Lactic dehydrogenase activity released by NVMs incubated with a synthetic DCD peptide (DCD 20–110) or a control peptide (CTR) under normoxic or hypoxic conditions (*$P<0.05$ vs. normoxia; **$P<0.05$ vs. all). (*E*) Representative immunoblots (left panels) and cumulative data (right panels) of three independent experiments to evaluate the levels of cleaved PolyADP-ribose polymerase (PARP), cleaved caspase 3 and GAPDH in NVMs under normoxic or hypoxic conditions incubated with a synthetic DCD peptide (DCD 20–110) or a control peptide (CTR; *$P < 0.05$ vs. normoxia; **$P < 0.05$ vs. all).

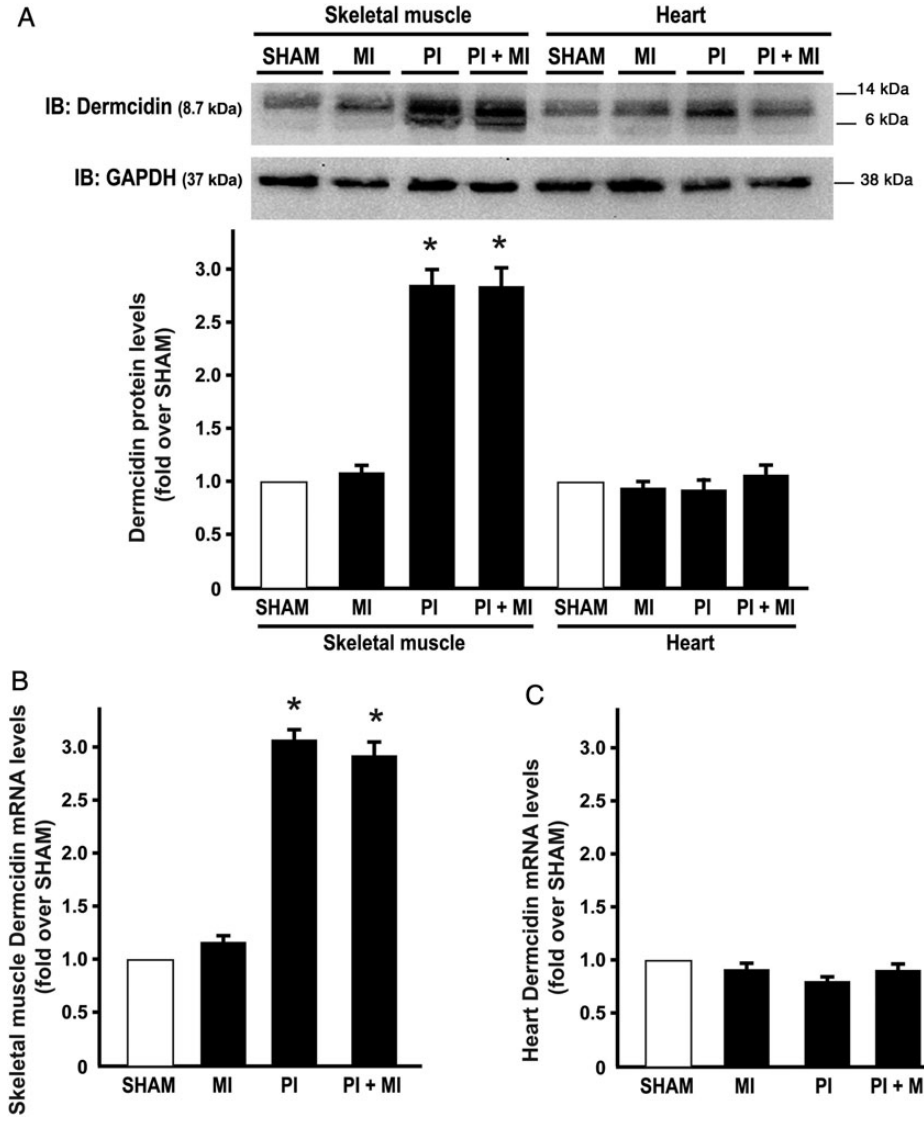

Figure 4 DCD expression in heart and skeletal muscle. (*A*) Representative immunoblot and densitometric analysis of four independent experiments to evaluate DCD protein levels in skeletal muscles or heart samples from SHAM, MI, PI, and PI + MI mice (*$P < 0.05$ vs. SHAM skeletal muscle; $n = 9$ tissues/group). GAPDH protein levels did not significantly change among the samples. (*B*) DCD mRNA levels in skeletal muscles from SHAM, MI, PI, or PI + MI (*$P < 0.05$ vs. SHAM; $n = 9$ tissues/group). (*C*) DCD mRNA levels in heart samples from SHAM, MI, PI, or PI + MI (not significant; $n = 9$ tissues/group).

the systemic circulation can enhance cardiomyocyte apoptosis and adverse cardiac remodelling induced by myocardial infarction. Interestingly, we never detected activation of the apoptotic cascade in normoxic cardiomyocytes incubated with DCD, suggesting that this peptide might have no direct toxic effects on these cells, but rather represents a novel, circulating factor that sensitizes, with an unknown mechanism, cardiomyocytes to an ischaemic insult. Consistently, the systemic delivery of specific DCD siRNA determined a significantly smaller infarct size area and a better cardiac function after coronary artery ligation, indicating DCD as a crucial factor in the modulation of cardiomyocytes survival under hypoxic conditions *in vitro* and *in vivo*. However, we cannot exclude that other important pathophysiological mechanisms might also be involved in the development of pathological remodelling and cardiac dysfunction under these experimental conditions.

In contrast to our results indicating DCD's detrimental effects on cardiomyocytes and the whole heart, in several solid tumours DCD has been demonstrated to induce cellular proliferation, migration, and survival during hypoxia.[29–31] However, DCD gene codes for a secreted precursor protein of 110 amino acid residues with a high susceptibility to proteolytic processing,[32] and while we found a full-length DCD protein in all our mass-spectrometry and proteomic analyses, several DCD products have been shown to be processed by neuronal cells or tumour cells. In particular, a peptide comprising the first 30 amino acids of the DCD precursor protein named Y-P30,[33] and another 20-amino-acid peptide derived from the N-terminal end of the DCD protein (proteolysis-inducing factor, PIF) exhibit a different range of biological functions despite large homologies in the amino acid sequences.[32] Whether DCD and/or its derived peptides interact with different target receptors is currently not

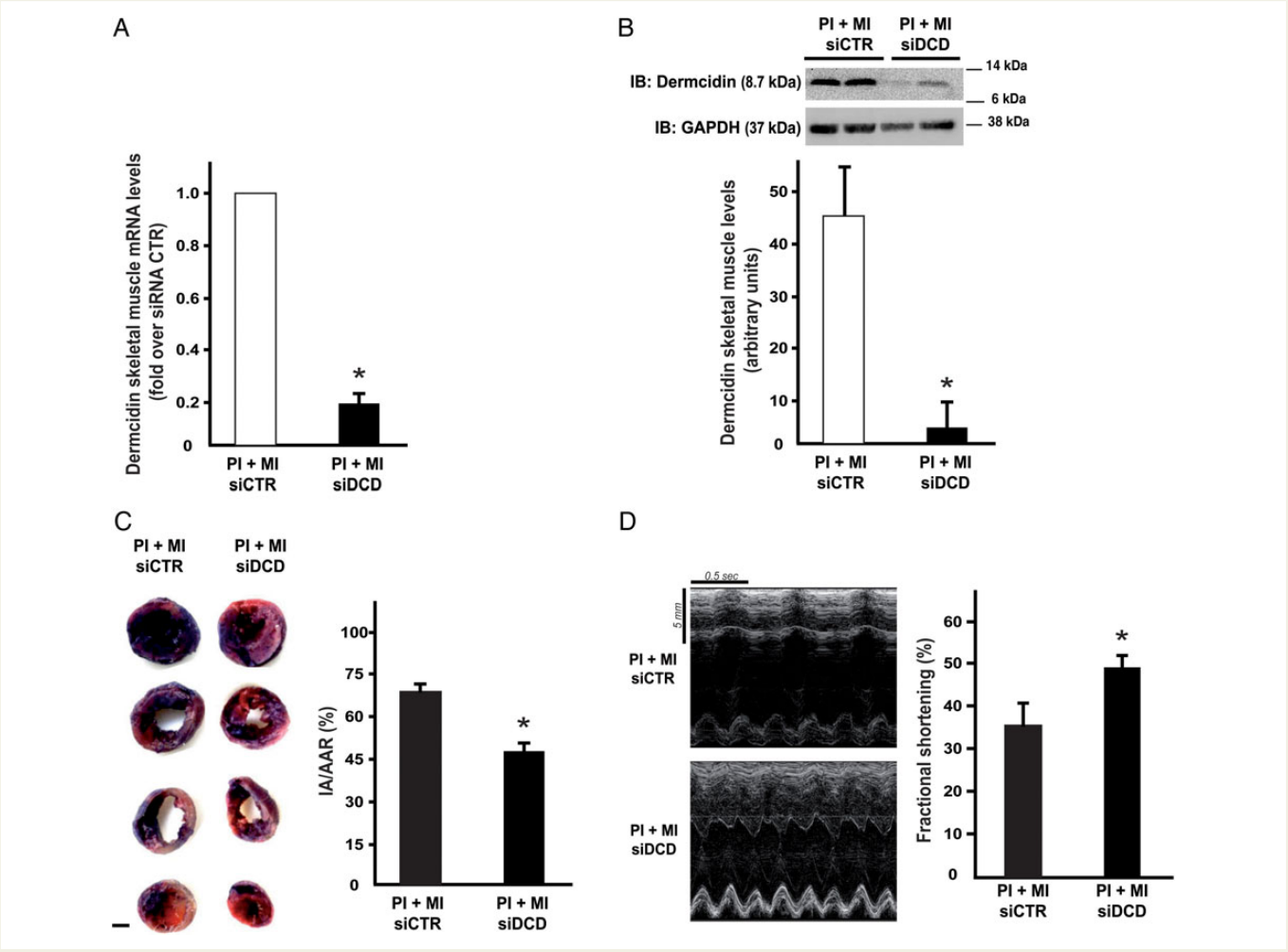

Figure 5 *In vivo* DCD interfering reduces infarct size and ameliorates cardiac remodelling. DCD mRNA (*A*) and protein levels (*B*) in skeletal muscle samples from PI + MI mice treated with control siRNA (PI + MI siCTR) or DCD siRNA (PI + MI siDCD) (*$P < 0.05$ vs. PI + MI siCTR; $n = 6$ tissues/group). Representative immunoblot and densitometric analysis of four independent experiments are reported (*$P < 0.05$ vs. PI + MI siCTR; $n = 6$ tissues/group). (*C*) Left: Representative images of triphenyltetrazolium chloride (TTC) staining of heart sections from PI + MI siCTR or PI + MI siDCD mice 24 h after coronary artery ligation (scale bar = 1 mm). Right: bar graphs showing ratios of myocardial infarct area (IA) vs. area at risk (AAR) in both groups (*$P < 0.05$ vs. PI + MI siCTR; $n = 6$ hearts/group). (*D*) Left: representative M-mode echocardiographic tracings and cumulative data (right) of % fractional shortening in PI + MI siCTR or PI + MI siDCD (*$P < 0.05$ vs. PI + MI siCTR; $n = 6$ hearts/group).

known. In addition, it has been demonstrated that human DCD is phosphorylated at Tyr[23] and polymethylated at Lys,[34] further complicating the possibility of associating an exact molecular mass to a specific peptide form.

In summary, this study identifies a novel biochemical mechanism of remote 'crosstalk' between skeletal muscle and the heart, based on the molecular actions of a novel detrimental myokine, i.e. DCD. These results might explain, at least in part, the important association between LE-PAD and cardiovascular mortality and morbidity.[3,4] These results might have important clinical implications in patients with diffuse vascular disease, since they suggest that treatment of peripheral artery disease, in addition to the amelioration of limb perfusion and function, might also significantly improve cardiovascular outcome, as also suggested by recent clinical observations.[35] Thus, our data configure DCD as a novel possible biomarker for LE-PAD and a novel exciting therapeutic target to reduce heart failure development and progression in patients with diffuse vascular arterial disease.

Supplementary material

Supplementary material is available at *Cardiovascular Research* online.

Acknowledgements

We decided to dedicate this manuscript to the memory of Massimo Chiariello MD.

Conflict of interest: none declared.

Funding

This study was supported in part by grant from Programma Operativo Nazionale (PON) – Ricerca e Competitività 2007–2013 'CARDIOTECH – TeCnologie Avanzate per l'innovazione e 1'Ottimizzazione dei pRocessi DIagnOstici, Terapeutici E di training dedicati alla gestione Clinica, interventistica e riabilitativa dei paziente affetti da sindromi coronaricHe acute' (PON01_02833) to G.E., by grants from the Italian Ministry of Health –

Young Researcher Grant (2009) and from the Italian Ministry of University and Research – FIRB 2012 Grant (Futuro in Ricerca) to C.P., and by grant from Regione Campania to the Rete di Spettrometria di Massa della Campania - RESMAC to A.S.

References

1. Hansson GK. Inflammation, atherosclerosis, and coronary artery disease. *N Engl J Med* 2005;**352**:1685–1695.
2. Chiong M, Wang ZV, Pedrozo Z, Cao DJ, Troncoso R, Ibacache M, Criollo A, Nemchenko A, Hill JA, Lavandero S. Cardiomyocyte death: mechanisms and translational implications. *Cell Death Dis* 2011;**2**:e244.
3. Brevetti G, Piscione F, Schiano V, Galasso G, Scopacasa F, Chiariello M. Concomitant coronary and peripheral arterial disease: relationship between the inflammatory status of the affected limb and the severity of coronary artery disease. *J Vasc Surg* 2009;**49**: 1465–1471.
4. Criqui MH, Langer RD, Fronek A, Feigelson HS, Klauber MR, McCann TJ, Browner D. Mortality over a period of 10 years in patients with peripheral arterial disease. *N Engl J Med* 1992;**326**:381–386.
5. Papamichael CM, Lekakis JP, Stamatelopoulos KS, Papaioannou TG, Alevizaki MK, Cimponeriu AT, Kanakakis JE, Papapanagiotou A, Kalofoutis AT, Stamatelopoulos SF. Ankle-brachial index as a predictor of the extent of coronary atherosclerosis and cardiovascular events in patients with coronary artery disease. *Am J Cardiol* 2000;**86**: 615–618.
6. Erren M, Reinecke H, Junker R, Fobker M, Schulte H, Schurek JO, Kropf J, Kerber S, Breithardt G, Assmann G, Cullen P. Systemic inflammatory parameters in patients with atherosclerosis of the coronary and peripheral arteries. *Arterioscler Thromb Vasc Biol* 1999;**19**:2355–2363.
7. Brevetti G, Piscione F, Cirillo P, Galasso G, Schiano V, Barbato E, Scopacasa F, Chiariello M. In concomitant coronary and peripheral arterial disease, inflammation of the affected limbs predicts coronary artery endothelial dysfunction. *Atherosclerosis* 2008;**201**:440–446.
8. Pedersen BK, Akerstrom TC, Nielsen AR, Fischer CP. Role of myokines in exercise and metabolism. *J Appl Physiol (1985)* 2007;**103**:1093–1098.
9. Pedersen L, Hojman P. Muscle-to-organ cross talk mediated by myokines. *Adipocyte* 2012;**1**:164–167.
10. Curcio A, Noma T, Naga Prasad SV, Wolf MJ, Lemaire A, Perrino C, Mao L, Rockman HA. Competitive displacement of phosphoinositide 3-kinase from beta-adrenergic receptor kinase-1 improves postinfarction adverse myocardial remodeling. *Am J Physiol Heart Circ Physiol* 2006;**291**:H1754–H1760.
11. Stabile E, Burnett MS, Watkins C, Kinnaird T, Bachis A, la Sala A, Miller JM, Shou M, Epstein SE, Fuchs S. Impaired arteriogenic response to acute hindlimb ischemia in CD4-knockout mice. *Circulation* 2003;**108**:205–210.
12. Couffinhal T, Silver M, Zheng LP, Kearney M, Witzenbichler B, Isner JM. Mouse model of angiogenesis. *Am J Pathol* 1998;**152**:1667–1679.
13. Perrino C, Schiattarella GG, Sannino A, Pironti G, Petretta MP, Cannavo A, Gargiulo G, Ilardi F, Magliulo F, Franzone A, Carotenuto G, Serino F, Altobelli GG, Cimini V, Cuocolo A, Lombardi A, Goglia F, Indolfi C, Trimarco B, Esposito G. Genetic deletion of uncoupling protein 3 exaggerates apoptotic cell death in the ischemic heart leading to heart failure. *J Am Heart Assoc* 2013;**2**:e000086.
14. Krege JH, Hodgin JB, Hagaman JR, Smithies O. A noninvasive computerized tail-cuff system for measuring blood pressure in mice. *Hypertension* 1995;**25**:1111–1115.
15. Alfie ME, Sigmon DH, Pomposiello SI, Carretero OA. Effect of high salt intake in mutant mice lacking bradykinin-B2 receptors. *Hypertension* 1997;**29**:483–487.
16. Morisco C, Zebrowski D, Condorelli G, Tsichlis P, Vatner SF, Sadoshima J. The Akt-glycogen synthase kinase 3beta pathway regulates transcription of atrial natriuretic factor induced by beta-adrenergic receptor stimulation in cardiac myocytes. *J Biol Chem* 2000;**275**:14466–14475.
17. Esposito G, Perrino C, Schiattarella GG, Belardo L, di Pietro E, Franzone A, Capretti G, Gargiulo G, Pironti G, Cannavo A, Sannino A, Izzo R, Chiariello M. Induction of mitogen-activated protein kinases is proportional to the amount of pressure overload. *Hypertension* 2010;**55**:137–143.
18. Carnevale D, Cifelli G, Mascio G, Madonna M, Sbroggio M, Perrino C, Persico MG, Frati G, Lembo G. Placental growth factor regulates cardiac inflammation through the tissue inhibitor of metalloproteinases-3/tumor necrosis factor-alpha-converting enzyme axis: crucial role for adaptive cardiac remodeling during cardiac pressure overload. *Circulation* 2011;**124**:1337–1350.
19. Caratu G, Allegra D, Bimonte M, Schiattarella GG, D'Ambrosio C, Scaloni A, Napolitano M, Russo T, Zambrano N. Identification of the ligands of protein interaction domains through a functional approach. *Mol Cell Proteomics* 2007;**6**:333–345.
20. Gaziano TA, Bitton A, Anand S, Abrahams-Gessel S, Murphy A. Growing epidemic of coronary heart disease in low- and middle-income countries. *Curr Probl Cardiol* 2010;**35**: 72–115.
21. Lu X, Hamilton JA, Shen J, Pang T, Jones DL, Potter RF, Arnold JM, Feng Q. Role of tumor necrosis factor-alpha in myocardial dysfunction and apoptosis during hindlimb ischemia and reperfusion. *Crit Care Med* 2006;**34**:484–491.
22. Schittek B, Hipfel R, Sauer B, Bauer J, Kalbacher H, Stevanovic S, Schirle M, Schroeder K, Blin N, Meier F, Rassner G, Garbe C. Dermcidin: a novel human antibiotic peptide secreted by sweat glands. *Nat Immunol* 2001;**2**:1133–1137.
23. Shen SL, Qiu FH, Dayarathna TK, Wu J, Kuang M, Li SS, Peng BG, Nie J. Identification of Dermcidin as a novel binding protein of Nck1 and characterization of its role in promoting cell migration. *Biochim Biophys Acta* 2011;**1812**:703–710.
24. Deans DA, Wigmore SJ, Gilmour H, Tisdale MJ, Fearon KC, Ross JA. Expression of the proteolysis-inducing factor core peptide mRNA is upregulated in both tumour and adjacent normal tissue in gastro-oesophageal malignancy. *Br J Cancer* 2006;**94**:731–736.
25. Stewart GD, Skipworth RJ, Pennington CJ, Lowrie AG, Deans DA, Edwards DR, Habib FK, Riddick AC, Fearon KC, Ross JA. Variation in dermcidin expression in a range of primary human tumours and in hypoxic/oxidatively stressed human cell lines. *Br J Cancer* 2008;**99**:126–132.
26. Stocki P, Wang XN, Morris NJ, Dickinson AM. HSP70 natively and specifically associates with an N-terminal dermcidin-derived peptide that contains an HLA-A*03 antigenic epitope. *J Biol Chem* 2011;**286**:12803–12811.
27. Ghosh R, Maji UK, Bhattacharya R, Sinha AK. The role of dermcidin isoform 2: a two-faceted atherosclerotic risk factor for coronary artery disease and the effect of acetyl salicylic Acid on it. *Thrombosis* 2012;**2012**:987932.
28. Ghosh R, Karmohapatra SK, Bhattacharyya M, Bhattacharya R, Bhattacharya G, Sinha AK. The appearance of dermcidin isoform 2, a novel platelet aggregating agent in the circulation in acute myocardial infarction that inhibits insulin synthesis and the restoration by acetyl salicylic acid of its effects. *J Thromb Thrombolysis* 2011;**31**:13–21.
29. Stewart GD, Skipworth RJ, Ross JA, Fearon K, Baracos VE. The dermcidin gene in cancer: role in cachexia, carcinogenesis and tumour cell survival. *Curr Opin Clin Nutr Metab Care* 2008;**11**:208–213.
30. Chang WC, Huang MS, Yang CJ, Wang WY, Lai TC, Hsiao M, Chen CH. Dermcidin identification from exhaled air for lung cancer diagnosis. *Eur Respir J* 2010;**35**: 1182–1185.
31. Stewart GD, Lowrie AG, Riddick AC, Fearon KC, Habib FK, Ross JA. Dermcidin expression confers a survival advantage in prostate cancer cells subjected to oxidative stress or hypoxia. *Prostate* 2007;**67**:1308–1317.
32. Lowrie AG, Dickinson P, Wheelhouse N, Stewart GD, Ross AJ, Forster T, Ross JA. Proteolysis-inducing factor core peptide mediates dermcidin-induced proliferation of hepatic cells through multiple signalling networks. *Int J Oncol* 2011;**39**:709–718.
33. Porter D, Weremowicz S, Chin K, Seth P, Keshaviah A, Lahti-Domenici J, Bae YK, Monitto CL, Merlos-Suarez A, Chan J, Hulette CM, Richardson A, Morton CC, Marks J, Duyao M, Hruban R, Gabrielson E, Gelman R, Polyak K. A neural survival factor is a candidate oncogene in breast cancer. *Proc Natl Acad Sci USA* 2003;**100**: 10931–10936.
34. Choudhary C, Kumar C, Gnad F, Nielsen ML, Rehman M, Walther TC, Olsen JV, Mann M. Lysine acetylation targets protein complexes and co-regulates major cellular functions. *Science* 2009;**325**:834–840.
35. Giugliano G, Di Serafino L, Perrino C, Schiano V, Laurenzano E, Cassese S, De Laurentis M, Schiattarella GG, Brevetti L, Sannino A, Gargiulo G, Franzone A, Indolfi C, Piscione F, Trimarco B, Esposito G. Effects of successful percutaneous lower extremity revascularization on cardiovascular outcome in patients with peripheral arterial disease. *Int J Cardiol* 2013;**167**:2566–2571.